Proceeding of the 2004 American Control Conference
Boston, Massachusetts June 30 - July 2, 2004

Reduced Order Control in Microchemical Systems

Leonidas G. Bleris and Mayuresh V. Kothare

Abstract— **In this paper we examine the problem of regulation of thermal transients in a microsystem. Using second-order statistical properties we obtain the dominant structures that characterize the dynamics of an ensemble of data. These dominant structures, otherwise called empirical eigenfunctions, are the most efficient way of capturing the dynamics of an infinite dimensional process with a finite number of modes. We propose a new receding horizon boundary control scheme using these empirical eigenfunctions in a constrained optimization procedure to track a desired spatiotemporal profile. Additionally we consider a disturbance rejection problem. Finite element method simulations of heat transfer are provided and used in order to implement and test the performance of the controller.**

I. INTRODUCTION

ONE of the most active research areas of the past decade is the Systems-on-a-Chip (SoC) applications. Evolving from simple prototype applications, novel more sophisticated SoC are currently being developed for a variety of applications. The SoC market is expanding rapidly to areas like bioengineering (DNA analysis and synthesis, drug delivery), avionics and aerospace (microactuators, microsensors and microgyroscopes) and automotive systems (accelerometers). A new generation of SoC are the integrated microchemical systems [1], [2], [3]; miniature chemical systems that carry out chemical reactions and separations in microreactor configurations in the size range of a few microns to a few hundred microns. The main focus of research in microchemical systems remains on the micro-fabrication aspects. As a result, there is very little work in the literature on the dynamics and control of these highly functional and versatile SoC. Applying control in a microchemical system may include efficient mixing of different laminar streams, manipulating microflows and adjusting the temperature distribution of the microsystem. The system states such as temperature, concentration, pressure and velocity are functions of space and time. Thus we have Distributed Parameter Systems (DPS) [4] with combined distributed boundary sensing and actuation. From a control perspective we face the following challenges. Firstly the development of an efficient controller capable of handling the high dimensional models of these SoC and secondly reducing its complexity so that it can be implemented on a chip and subsequently embedded with the rest of the system.

Due to the low Reynolds number flows encountered in microsystems, mixing of adjacent streams occurs primarily by diffusion. To decrease the mixing length and time, transverse streams must be created within the microchannels. This is mainly accomplished using passive control methods; by creating appropriate geometries to enhance the mixing [5], [6]. There are also reports on active methods of creating transverse flows, by using mechanical oscillating components on the microchannel walls or introducing flows via side channels. Manipulating microflows can be achieved by applying control both on the macroscopic level or within the microchannel. The simplest approach is applying control on specific inlets and outlets on the macroscopic level. Within the microchannels control can be applied using different kinds of external fields. There are applications that use electric fields, magnetic forces, sound and capillary effects [7]. Some initial research efforts have been reported on controlling the temperature distribution in microchemical systems [8]. We have previously [9] used Finite Element Method (FEM) simulations of heat transfer of microchannels coupled with the use of SIMULINK as a framework for the application of Proportional Integral (PI) and On/Off control. We are currently investigating ways of embedding model predictive control for the application of optimal control in SoC applications [10].

In this paper we propose to employ general principles from Proper Orthogonal Decomposition (POD) theory, derived from the control of distributed parameter systems [11], [12], in order to provide a novel reduced order boundary control scheme. In [13] we proposed an off-line control scheme based on POD of the temperature profiles obtained by FEM simulations. In [14] we examined an on-line open-loop boundary control scheme using the POD based empirical eigenfunctions of a spatiotemporal profile. In this work we extend the above ideas. In order to reduce the size of the control problem of regulating the temperature in a microsystem we use spatial and temporal empirical eigenfunctions, that characterize the dominant dynamics of the process. In contrast to proposed approaches these eigenfunctions are used without the usually subsequent Galerkin projection, that would yield a system of Ordinary Differential Equations (ODEs). We propose a novel receding horizon boundary control scheme using the empirical eigenfunctions in a constrained optimization procedure, that results in the desired spatiotemporal profile.

This paper is organized as follows. Section II contains a brief analysis of the theoretical aspects of the proposed approach. Details on the examined micro-geometry and the

Partial financial support for this research from the US National Science Foundation under grants CTS-9980781 (“Engineering Microsystems: XYZ-on-a-chip” program) and CTS-0134102 (CAREER program) is gratefully acknowledged.

Mayuresh V. Kothare is with the Faculty of Chemical Engineering, Lehigh University, Bethlehem, PA, 18015 mayuresh.kothare@lehigh.edu

Leonidas G. Bleris is with the Department of Electrical and Computer Engineering, Lehigh University, Bethlehem, PA, 18015 leb3@lehigh.edu

0-7803-8335-4/04/$17.00 ©2004 AACC

heat transfer model are given in Section III. In Section IV we provide the closed-loop receding horizon eigenfunction based controller. We analyze the reason for introducing constraints on the boundary actuation and we examine the performance of this control approach under external disturbances.

II. Theoretical Aspects

A mathematical method which has received growing attention lately, is proper orthogonal decomposition. POD is the most efficient way of capturing the dominant components of an infinite dimensional process with a finite number of modes [15]. Let $Y \in \Re^{N\times M}$ be the matrix that contains data collected from experimental results or simulations. The value of this matrix at row t and column x is represented by the scalar $y_t(x)$. Thus we have N observations (called snapshots) of some ergodic physical process taken at positions x, where $x = 1, ..., M$. The aim of POD is to find the most representative structure $\varphi(x)$ of this ensemble of snapshots. This is equivalent to maximizing the averaged projection of φ onto y

$$\underset{\varphi}{max}\{\lambda = \frac{\langle(\varphi, y)^2\rangle}{(\varphi,\varphi)}\} \tag{1}$$

A necessary condition for (1) to hold is that φ is an eigenfunction of the two-point correlation function

$$\int_{\Omega}\frac{1}{N}\sum_{t=1}^{N} y_t(x)y_t(x')\varphi(x')dx' = \lambda\varphi(x) \tag{2}$$

This integral equation can be solved by means of the Hilbert-Schmidt [16] technique or the method of snapshots [17] (practical when the number of observations N is less than the discretization M). For the method of snapshots we assume that the eigenfunctions are a linear combination of the snapshots

$$\varphi(x) = \sum_{t=1}^{N}\alpha_t y_t(x) \tag{3}$$

The solution of (2) is reduced to the eigenvalue problem of $C_{ij}V = \lambda V$, where C is a Hermitian matrix, in the discrete case given by

$$C_{ij} = \frac{1}{N}\sum_{x=1}^{M} y_i(x)y_j(x) \quad\quad i,j = 1, ..., N \tag{4}$$

The projection of $\varphi(x)$ onto $y_t(x)$ is maximized when the coefficients α are the elements of the eigenvector V that corresponds to the largest eigenvalue of C. The eigenfunction that corresponds to the first eigenvector is considered to be the most “energetic”. The “energy” is defined as being the sum of the eigenvalues of the matrix C, and to each eigenfunction we assign an “energy” percentage based on the eigenfunction’s associated eigenvalue

$$E_k = \frac{\lambda_k}{\sum_{i=1}^{N}\lambda_i} \tag{5}$$

There is no a priori framework for the generation of the ensemble, but a basic assumption generally made is that the snapshots are fully representative of the temporal evolution of the system. In this work we assume that the data ensemble represents the dynamics of the system perfectly both temporally and spatially. Under this assumption we obtain two families of empirical eigenfunctions. One family that characterizes the changes in the spatial profile (the spatial eigenfunctions ϕ) and one the characterizes changes in time (the temporal eigenfunctions ψ). Using the method of snapshots the problem of obtaining the spatial eigenfunctions is reduced to finding the eigenvalues and eigenvectors of the $N \times N$ matrix C_s

$$(C_s)_{ij} = \frac{1}{N}\sum_{x=1}^{M} y_i(x)y_j(x) \quad\quad i,j = 1, ..., N \tag{6}$$

The eigenvectors $A^{(n)}$ of C_s and the corresponding eigenvalues λ_n^s satisfy

$$C_s A^{(n)} = \lambda_n^s A^{(n)} \quad\quad n = 1, ..., N \tag{7}$$

The empirically determined spatial eigenfunctions $\phi_k(x)$ are then computed using the obtained eigenvectors using

$$\phi_k(x) = \sum_{i=1}^{N} A_i^{(k)} y_i(x) \tag{8}$$

In order to calculate the temporal eigenfunctions ψ (when working in $1D$ in space and in time), we take the transpose of the initial snapshot matrix Y and we obtain an adjusted data set $\tilde{Y}$, where $\tilde{Y}$ is now an $M \times N$ matrix. The scalar $\tilde{y}_t(x)$ represents the value of $\tilde{Y}$ at row t and column x, where $t = 1, ..., M$ and $x = 1, ...N$. Using this ensemble we apply the method of snapshots (analytically in [18]). To obtain the Hermitian matrix (now $M \times M$) we use

$$(C_t)_{ij} = \frac{1}{M}\sum_{x=1}^{N} \tilde{y}_i(x)\tilde{y}_j(x) \quad\quad i,j = 1, ..., M \tag{9}$$

and the temporal eigenfunctions $\psi_k(t)$ are given by

$$\psi_k(t) = \sum_{i=1}^{M} B_i^{(k)} \tilde{y}_i(t) \tag{10}$$

where $B^{(n)}$ are the eigenvectors of C_t.

III. Geometry Examined

With the rapid development of computers and the software tool capabilities, SoC applications can be examined through advanced simulation techniques. We use FEMLAB [19], a Partial Differential Equation (PDE) solver. With FEMLAB one can build 3D geometries and define the equations that describe the dynamics of the system. Consider Fig. 1 which shows a wafer geometry, with thin film resistive heaters placed on the top wall. The wafer states such as temperature are functions of space and time. Thus, this is a distributed parameter system with

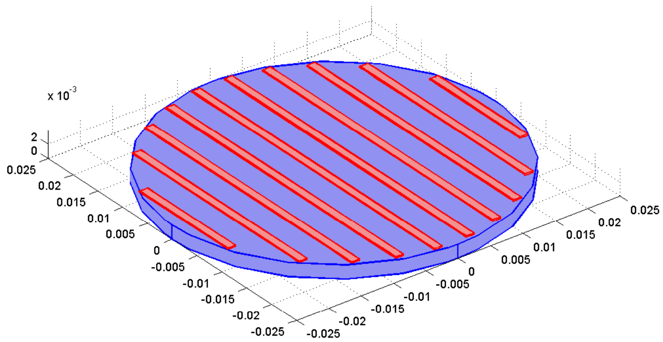

Fig. 1. 3D Wafer Geometry (dimensions in meters)

combined distributed and boundary sensing and actuation. We note that this system is inherently distributed, as opposed to a number of reported studies on systems that are distributed because they are comprised of distributed interacting systems. Because of the increasing complexity of microchemical systems we often desire to have spatiotemporal differences in temperature within the same SoC usually built on a wafer. This can be partially achieved with the use of low thermal conductivity materials coupled with the use of thermal barriers and insulations but the application of control is essential. In the following section we examine the temperature distribution in the cross section of the wafer shaped rectangular geometry of 5cm width and 2mm thickness, as illustrated in Fig. 2. Ten resistive heaters are placed on top and we have ten temperature sensors, on equally spaced nodes of the finite element mesh located at the bottom of the geometry. The temperature distribution in

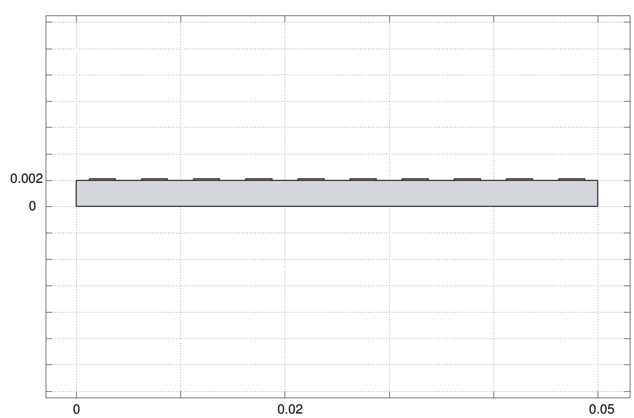

Fig. 2. Geometry examined

the wafer cross section is described by the time-dependent two dimensional heat equation

$$\frac{\partial T(t,x,y)}{\partial t} = \frac{1}{a}\nabla^2 T(t,x,y) \qquad (11)$$

where $a = \rho C/\kappa$, κ is the thermal conductivity, ρ is the density and C is the heat capacity. We consider natural convection for boundary conditions (T_{air}=300K and h=25W/m^2K) and initial condition of $T(0,x,y) = 300$K. The material used for the FEM simulations is ceramic.

IV. Receding Horizon Eigenfunction Based Controller

Generally controllers belonging to the Receding Horizon Control (RHC) family [20] are characterized by the following steps. Initially the future outputs are calculated at each sample interval over a predetermined horizon N, the prediction horizon, using the process model. These outputs $y(t+k|t)$ for k =1,...,N depend up to the time t on the past inputs and on the future signals $u(t+k|t)$, k=0,...,N-1 which are those to be sent to the system. The next step is to calculate the set of future control moves by optimizing a determined criterion in order to keep the process as close as possible to a predefined reference trajectory. Finally, the first control move $u(t|t)$ is sent to the system while the rest are rejected. This is because at the next sampling instant the output $y(t+1)$ is measured and the procedure is repeated with the new values so that we get an updated control sequence.

In order to implement this strategy for our problem using the empirical eigenfunctions we have to make some adjustments. The model used to predict the future outputs is a FEMLAB created model. We provide an initial input

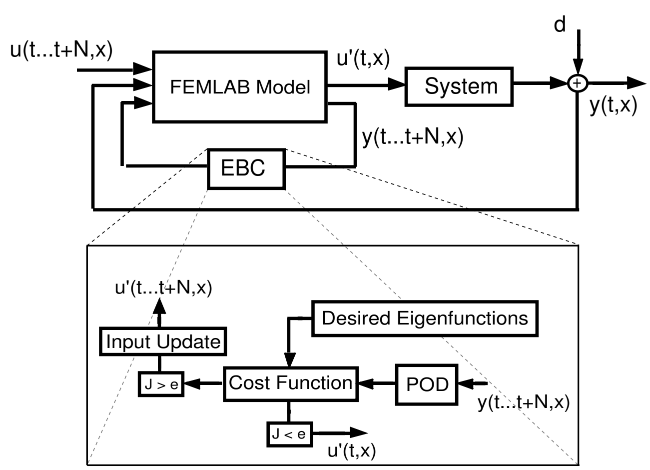

Fig. 3. Receding horizon controller block diagram

to the system $u_{(t+k|t)}(x)$, where $k = 0,...,N-1$ (N is the prediction and control horizon) and $x = 1,...,M$ (M are the spatially distributed points). The output of the FEM model $y_t(x)$, measured at the locations of the distributed sensors, undergoes POD for the calculation of the dominant empirical temporal and spatial eigenfunctions. For both of the above families of eigenfunctions we keep the most “energetic” eigenfunctions. These dominant spatial and temporal eigenfunctions are then used in objective functions that consist of the difference of the current and the desired dominant eigenfunctions

$$J_t(u) = \sum_{t=1}^{N} |\psi_1(t) - \psi_1^d(t)| \tag{12}$$

and

$$J_s(u) = \sum_{x=1}^{M} |\phi_1(x) - \phi_1^d(x)| \tag{13}$$

The dominant temporal and spatial empirical eigenfunctions are given by

$$\phi_1(x) = \sum_{i=1}^{N} A_i^1 y_i(x) \tag{14}$$

and

$$\psi_1(t) = \sum_{i=1}^{M} B_i^1 \tilde{y}_i(t) \tag{15}$$

and the $\psi_1^d(t)$ and $\phi_1^d(x)$ are pre-calculated from the desired spatiotemporal profile. In order to be able to use these eigenfunctions in the proposed optimization procedure we have to directly relate them to the boundary actuation u. From (14) and (15) we can conclude that to be able to steer the eigenfunctions to a desirable reachable state we need to obtain further information for the eigenvectors A_i^1 and B_i^1. A change in the boundary actuation will result in a relative change in the temperature output and subsequently to new Hermitian covariance matrices. We assume that small changes on the boundary actuation result in new matrices C_s' and C_t' which can be considered as a perturbation of the initial matrices C_s and C_t by H_s and H_t respectively.

At this point we can use the theory on perturbation of Hermitian matrices in order to calculate the bound on the boundary actuation that will assure that the most dominant eigenvectors of the new matrices C_s' and C_t' remain invariant. The difference between the subspace spanned by the eigenvectors of a Hermitian matrix and its perturbation can be expressed in terms of certain angles, through which one subspace must be rotated in order to reach the other. This angle can be calculated using the $tan2\theta$ theorem [21] for an eigenvalue and eigenvector pair. An alternative would be to directly calculate the angle between the dominant eigenvectors V′ and V of the perturbed and initial matrix respectively. This of course requires the solution of an eigenvalue problem for the eigenvectors at each optimization cycle introducing further computational costs. We chose to impose an empirically derived constraint on the boundary actuation that is expected to leave the dominant eigenvectors of the initial and perturbed matrices invariant. With the use of simulations we concluded that for the examined wafer system the bound for the boundary actuation that leaves the dominant eigenvectors invariant is applying changes up to 1W/m^2. As a consequence based on (14) and (15) we conclude that we can achieve a monotonic relationship between the changes on the boundary and the resulting most dominant eigenfunction. This observation is used in the optimization procedure required by the control algorithm. By imposing this constraint we are able to drive the most dominant eigenfunction to any desired reachable temperature, by adjusting accordingly the boundary energy supply.

As illustrated in Fig. 3 we have a closed loop controller. When the optimization for the first receding horizon window is complete, the first calculated boundary actuation input is implemented on the actual system. The response of the actual system to this input is then used as the starting points at the next sampling time instead of the FEMLAB model output, thereby providing feedback. The procedure is repeated moving the control horizon ahead in time.

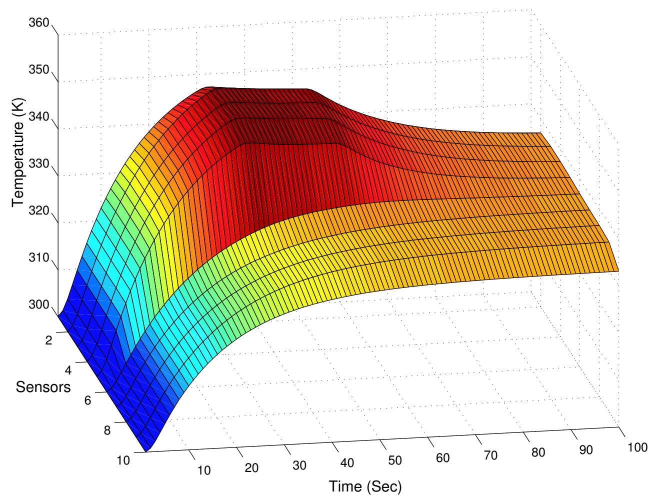

Fig. 4. Desired temperature profile

By minimizing the cost functions of (12) and (13) we want to steer the profile to the desired one (Fig. 4). The overall algorithm is as follows:

Receding Horizon Eigenfunction Based Control (EBC) Algorithm

Select the tolerance $\varepsilon > 0$, horizon N, compute desired spatial and temporal dominant eigenfunctions and perform the following steps:

Step 1: Give initial input to the model.

Step 2: Compute snapshots and associated spatial and temporal dominant eigenfunctions.

Step 3: Compute cost functions of (12) and (13). If both are less than ε go to Step 5.

Step 4: Adjust the boundary actuation u under the constraint of invariant eigenvectors until both cost functions are less than ε. If θ is not close to zero, decrease the boundary actuation.

Step 5: Implement the first computed boundary actuation input on the actual system, move the control horizon one sample ahead and go to Step 2.

A. Simulation Results

We use as set-point the temperature profile of Fig. 4. In order to test the proposed receding horizon approach we initially chose to use 30 seconds as the receding horizon, and we assume no external disturbances. The boundary actuation has the upper constraint of $10\text{W}/m^2$. Initially we provide $5\text{W}/m^2$ and we obtain temperature profiles from FEM simulations. Subsequently the energy supply is adjusted in order to minimize the cost functions J_s and J_t. Applying the proposed receding horizon algorithm we successfully drive the dominant eigenfunctions to the desired states (Fig. 5). Although we consider only the dominant eigenfunctions in the objective functions we notice that all of the first three spatial and temporal eigenfunctions are in good agreement.

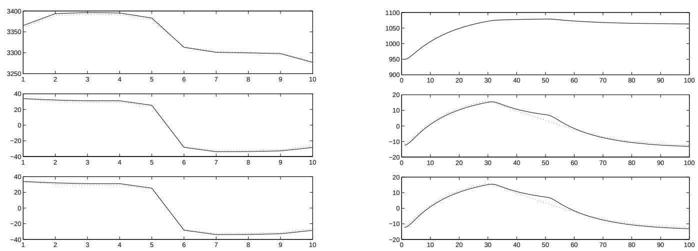

(a) (b)

Fig. 5. First three (a) spatial and (b) temporal eigenfunctions for receding horizon of 30 (Solid line: desired values - Dotted line: resulting values)

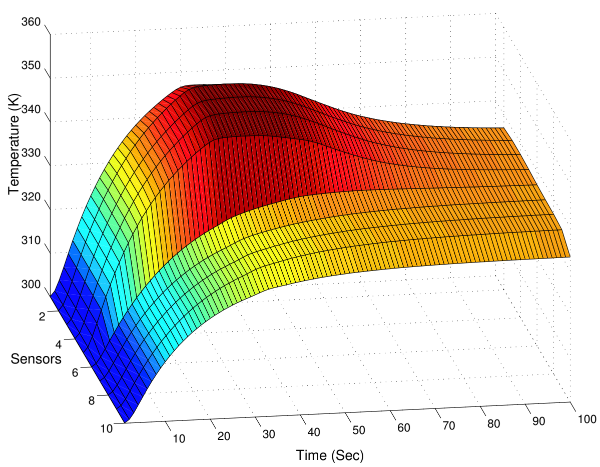

Fig. 6. Resulting temperature profile for receding horizon of 20

Using a control horizon of 20 the results can be further improved. From Fig. 7 and Fig. 8 we observe that the second and third spatial and temporal eigenfunctions are closer than these of using control horizon of 30. The resulting temperature profile is given in Fig. 6. We have to note here that there is a trade off in the accuracy of POD and the choice of less snapshots. Therefore one should proceed with caution choosing the window size in order not to sacrifice the efficiency of POD in capturing the dynamics of the system.

B. Disturbance Rejection

In this subsection we consider a disturbance rejection problem. We suppose that at time 65 seconds the ambient temperature changes to 320K; this results in a disturbance at the system output. As shown in Fig. 10, the receding horizon EBC is able to reject this disturbance by adjusting accordingly the boundary actuation. The open-loop EBC [14] is unable to recover the prescribed performance.

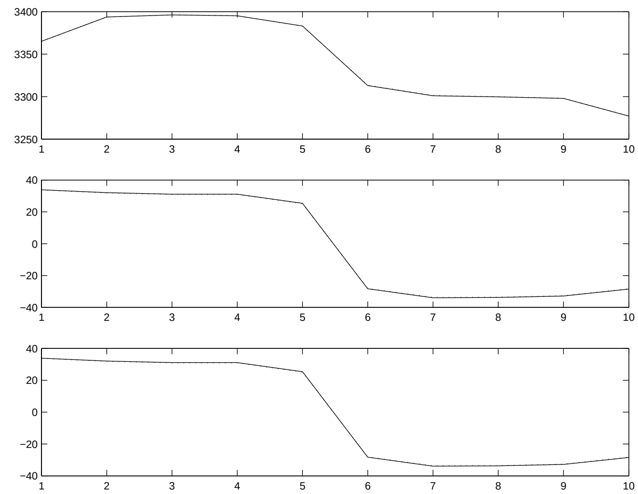

Fig. 7. First three spatial eigenfunctions for receding horizon of 20 (Solid line: desired values - Dotted line: resulting values)

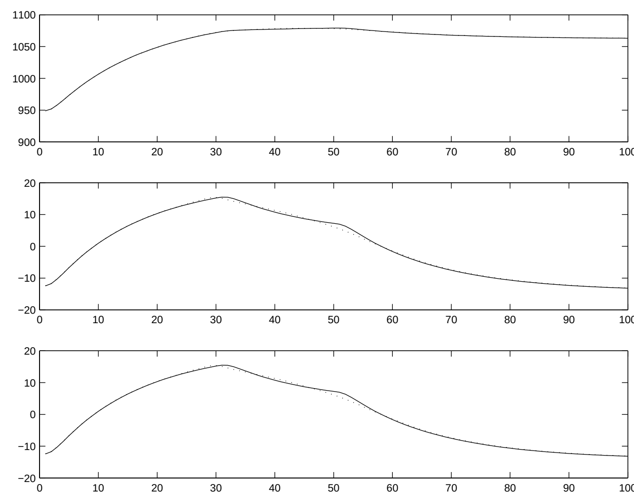

Fig. 8. First three temporal eigenfunctions for receding horizon of 20 (Solid line: desired values - Dotted line: resulting values)

V. Concluding Remarks

The application of a novel receding horizon eigenfunction based control scheme has been examined in this paper. Our extensive simulation experiments suggest that the application of this empirical eigenfunction based controller is most promising. Due to the novelty of the proposed idea there are open problems for further investigation.

For the formulation of the proposed control schemes we used the empirical eigenfunctions, that represent the dynamics of the heat transfer in the examined geometry. The minimization of the cost functions that consist of the spatial

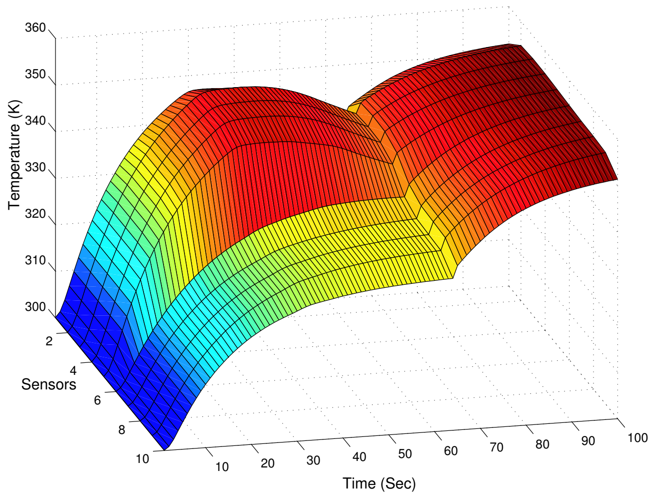

Fig. 9. Resulting temperature profile in presence of disturbance using open-loop EBC algorithm

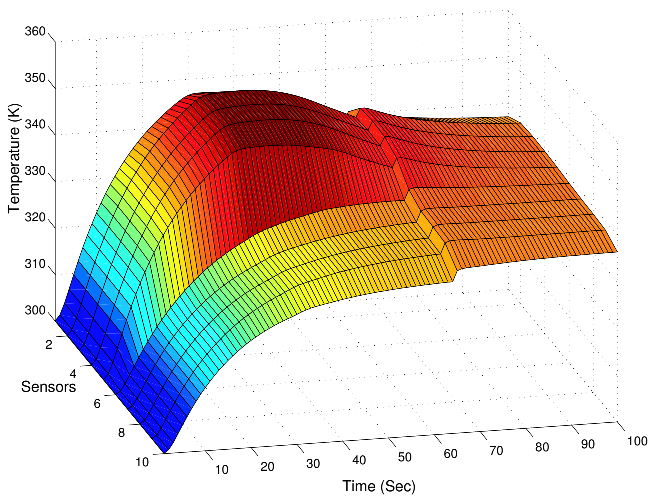

Fig. 10. Resulting temperature profile in presence of disturbance using closed-loop receding horizon EBC algorithm

and temporal eigenfunctions was achieved by a constrained move of the manipulated variables, in our case the boundary energy supply. It would be valuable to examine algorithms that utilize all of the POD-based empirical eigenfunctions in a multiple optimization problem. More specifically when the first eigenfunction does not contain 99% of the "energy" of the system we want to use a sufficient number of eigenfunctions in a cost function to capture this energy.

This novel receding horizon controller was applied for the regulation of temperature transients in a wafer-like cross section. Our analytical work and simulation results show that the proposed approach can provide an efficient reduced order boundary control method for even more complicated physical problems. In this direction, we are currently working on analyzing the stability and convergence properties of the proposed algorithm and applying the formulation to more complex microchemical systems that incorporate fluid flow and reactions.

References

[1] A. S. Pattekar and M. V. Kothare. A microreactor for hydrogen production in micro-fuel cell applications. *Journal of Microelectromechanical Systems*, February 2004.

[2] K. F. Jensen. Microchemical systems: Status, challenges and opportunities. *AIChE Journal*, 45(10):2051–2054, October 1999.

[3] D. L. Brenchley and R. S. Wegeng. Status of microchemical systems development in the United States of America. In *IMRET 2: Proceedings of the 2^{nd} International Conference on Microreaction Technology*, pages 18–23, 1998.

[4] P. D. Christofides. Control of nonlinear distributed process systems: Recent developments and challenges. *AIChE Journal*, 47(3):514–518, March 2001.

[5] M. W. Losey, R. J. Jackman, S. L. Firebaugh, M. A. Schmidt, and K. F. Jensen. Design and fabrication of microfluidic devices for multiphase mixing and reaction. *Journal of Microelectromechanical Systems*, 11(6):709–717, December 2002.

[6] A. D. Stroock, S. K. W. Dertinger, A. Ajdari, I. Mezic, H. A. Stone, and G. M. Whitesides. Chaotic mixer for microchannels. *Science*, 295:647–650, January 2002.

[7] H. A. Stone, A. D. Stroock, and A. Ajdari. Engineering flows in small devices: Microfluidics toward a lab-on-a-chip. *Annual Review of Fluid Mechanics*, 36:381–411, 2004.

[8] W. E. TeGrotenhuis, D. L. King, and K. P. Brooks. Optimizing microchannel reactors by trading-off equilibrium and reaction kinetics through temperature management. In *IMRET 6: Proceedings of the 6^{th} International Conference on Microreaction Technology*, 2002.

[9] L. G. Bleris and M. V. Kothare. Finite element method simulations of microchannels for control and reduced order modeling applications. In *Proceedings of the First International Conference on Mathematics and Informatics for Industry*, pages 162–169, Thessaloniki, Greece, April 2003.

[10] L. G. Bleris, M. V. Kothare, J. G. Garcia, and M. G. Arnold. Embedded model predictive control for system-on-a-chip applications. In *DYCOPS*, Boston, MA, July 2004.

[11] A. Armaou and P. D.Christofides. Optimization of dynamic transport-reaction systems using nonlinear model reduction. *Chemical Engineering Science*, 57:5083–5114, 2002.

[12] S. Y. Shvartsman and I. G. Kevrekidis. Nonlinear model reduction for control of distributed parameter systems: A computer assisted study. *AIChE Journal*, 44:1579, 1998.

[13] L. G. Bleris and M. V. Kothare. Model based control of temperature distribution in integrated microchemical systems. In *Proceedings of the 2003 American Control Conference*, pages 1308–1313, Denver, CO, June 2003.

[14] L. G. Bleris and M. V. Kothare. Boundary control of thermal transients in microsystems using proper orthogonal decomposition. In *International Conference of Influence of Traditional Mathematics and Mechanics on Modern Science and Technology*, Messini, Greece, May 2004.

[15] J. L. Lumley. *Stochastic Tools in Turbulence*. Academic Press, New York, 1970.

[16] P. Holmes, J. L. Lumley, and G. Berkooz. *Turbulence, coherent structures, dynamical systems and symmetry*. Cambridge monographs on Mechanics. Cambridge University Press, 1996.

[17] L. Sirovich. Turbulence and the dynamics of coherent structures: I, II, III. *Quarterly of applied mathematics*, XLV:561–590, 1987.

[18] L. G. Bleris and M. V. Kothare. Reduced order distributed boundary control of thermal transients in microsystems via the use of empirical eigenfunctions. *submitted to: IEEE Transactions on Control Systems Technology*, 2004.

[19] COMSOL AB, Natick, MA. *FEMLAB Reference Manual*, November 2001.

[20] E. F. Camacho and C. Bordons. *Model Predictive Control*. Springer, New York, 1999.

[21] C. Davis and W. M. Kahan. The rotation of eigenvectors by a perturbation III. *SIAM Journal of Numerical Analysis*, 7(1):1–46, 1970.